Six-fermion calculation of intermediate-mass Higgs boson production at future e^+e^- colliders

Guido Montagna[1,2], Mauro Moretti[3], Oreste Nicrosini[2,1], Fulvio Piccinini[2,1]

[1] Dipartimento di Fisica Nucleare e Teorica, Università di Pavia, I-27100 Pavia, Italy (e-mail: montagna@pv.infn.it)
[2] INFN, Sezione di Pavia, I-27100 Pavia, Italy (e-mail: nicrosini@pv.infn.it, nicrosini@vxcern.cern.ch, piccinini@pv.infn.it)
[3] Dipartimento di Fisica, Università di Ferrara and INFN, Sezione di Ferrara, I-44100 Ferrara, Italy
  (e-mail: moretti@axpfe1.fe.infn.it)

Abstract. The production of an intermediate-mass Higgs boson in processes of the kind $e^+e^- \rightarrow$ 6 fermions at the energies of future linear colliders is studied. The recently developed and fully automatic algorithm/code `ALPHA` is used to compute the tree-level scattering amplitudes for the reactions $e^+e^- \rightarrow \mu^+\mu^-\tau^-\bar{\nu}_\tau u\bar{d}, \mu^+\mu^-e^-\bar{\nu}_e u\bar{d}$. The code has been interfaced with the Monte Carlo program `HIGGSPV/WWGENPV`, properly adapted to 6-fermion production, in order to provide realistic results, both in the form of cross sections and event samples at the partonic level. Phenomenological results, that incorporate the effects of initial-state radiation and beamstrahlung, are shown and commented, emphasizing the potentials of full six-fermion calculations for precise background evaluation as well as for detailed studies of the fundamental properties of the Higgs particle.

1 Introduction

The investigation of the mechanism of electroweak symmetry breaking through the search for the Higgs particle constitutes one the main tasks of the experiments at present and future colliders. Present-day efforts at LEP2 are expected to reach the mass limit $m_h \approx \sqrt{s} - 100$ GeV and therefore will be unable to pursue the search for the Higgs boson in the interesting range of intermediate mass, i.e. $M_Z \leq m_h \leq 2M_Z$. This mass interval is actually particularly attractive since a number of theoretical arguments [1], as well as fits to precision electroweak data [2], provide indication for a weakly-coupled Higgs boson lighter than, say, 200 GeV. On the other hand, the discovery of the Higgs boson in the intermediate-mass interval might pose severe problems at the future large hadron collider LHC, in spite of continuous progress in detector performances and research strategies [3] as well as in updating theoretical predictions [4].

From this point of view, the next-generation of e^+e^- linear colliders (NLC) could be of great help in the complementary search for a Higgs boson with intermediate mass, as well as in the determination of its fundamental properties and couplings to SM particles. At the NLC, for "moderate" centre of mass (c.m.) energies up to 0.5 TeV, the main production mechanism for the Higgs boson is the Higgs-strahlung process $e^+e^- \rightarrow ZH$. When considering the $M_H > 135\div140$ GeV range, the above Higgs-strahlung process gives rise to a six-fermion final state, originating from Z decaying into $f\bar{f}$ pairs and Higgs boson decaying predominantly into WW pairs, with the subsequent decay of each W into leptonic $l\nu_l$ or hadronic $u\bar{d}$ final states. Therefore, the full calculation of the rate of intermediate-mass Higgs boson production at the NLC faces with the problem of a full calculation of $2 \rightarrow 6$ scattering amplitudes, including Higgs signal and background processes in the electroweak theory. The same difficulty applies to other very important research streams of the NLC, namely $t\bar{t}$ and three-vector bosons production, that both generate six-fermion final states.

A few calculations of such processes have been very recently performed, and a short account of the existing approaches can be found in [5]. Although different in several computational and numerical aspects, all these strategies rely upon the calculation of the very large number of Feynman diagrams involved (of the order of hundreds), exploiting in particular the experience accumulated during the last few years in the computations of the processes $e^+e^- \rightarrow 4$ fermions developed for W−pair and "light" Higgs boson production at LEP2 [6–10]. Concerning these recent calculations of specific processes of the kind $e^+e^- \rightarrow 6$ fermions $(6f)$, in [11] the full set of diagrams for the semi-leptonic processes $e^+e^- \rightarrow e^-\bar{\nu}_e 4q$ and $e^+e^- \rightarrow \mu^-\bar{\nu}_\mu 4q$ has been computed and physical distributions of interest for *top*-quark and WWZ physics have been analyzed in detail. Similar calculations are in progress following a fully computerized approach for the automatic computation of the Feynman diagrams by means of the `GRACE` system [12]. Previous calculations of helicity amplitudes relative to multi-particle production processes

and relevant for collider phenomenology can also be found in the literature [13].

Here an alternative attack strategy to the problem is presented, using a theoretical algorithm (and the corresponding code) recently proposed in the literature and known as `ALPHA` [14]. For a given lagrangian, this algorithm, of iterative nature, allows to compute numerically, in a fully automatic way, the tree-level scattering amplitudes, without using the Feynman diagrams, and it turns out to be particularly powerful for the calculation of those processes involving a high number of final-state particles. The resulting code has already been applied with success to the calculation of the rates of multi-particle production reactions of interest for the LEP2 and NLC experimental programme, such as $e^+e^- \to 4$ fermions, $e^+e^- \to 4$ fermions$+\gamma$ [14,15] and $\gamma\gamma \to \bar{\nu}_e e^- u\bar{d}$ [16]. In particular, in the case of four-fermion production processes the numerical results obtained with `ALPHA` have been compared in detail with those of independent formulations based on standard computational techniques, showing excellent agreement and thus providing a stringent test of the algorithm and of the resulting code [7,9]. In order to produce realistic results, the algorithm has been interfaced with the Monte Carlo program `HIGGSPV/WWGENPV` [17,18], developed for WW and Higgs boson physics in processes with four fermions in the final state in the context of LEP2 physics [19], and properly adapted to $6f$ production. The computational tool developed can work both as an integrator of weighted events, providing cross sections for any given experimental set up, and as a generator of unweighted events, providing event samples suited for physics analysis and/or detector simulation.

To the best of the authors' knowledge, a full six-fermion calculation of intermediate-mass higgs boson production in e^+e^- collisions and relative phenomenological analysis has not yet been performed. In this paper the results obtained for two different channels are presented, trying to emphasize the usefulness of a complete $6f$ calculation from the point of view of precise background evaluations in Higgs boson searches as well as for the determination of the fundamental properties (mass, spin, etc.) of this particle. Recent reviews on the main aspects of Higgs boson phenomenology at future e^+e^- linear colliders can be found in [20–25]. Moreover, also full calculations for processes of the kind $e^+e^- \to bbWW$, $bbZZ$ and $4jets + W$, of interest for Higgs boson searches at NLC, but with on shell final-state vector bosons, can be found in [26,27].

The paper is organized as follows. In Sect. 2, the details of the calculation are presented, considering intermediate-mass Higgs boson production in the six-fermion reactions $e^+e^- \to \mu^+\mu^-\tau^-\bar{\nu}_\tau u\bar{d}, \mu^+\mu^-e^-\bar{\nu}_e u\bar{d}$; a sample of illustrative numerical results is shown and commented in Sect. 3 and the main conclusions as well as possible perspectives are drawn in Sect. 4.

2 Six-fermion calculation

In order to study the intermediate-mass Higgs boson production at the NLC in channels that are as free as possible

from large background contamination, only the processes

$$e^+e^- \to \mu^+\mu^-\tau^-\bar{\nu}_\tau u\bar{d}, \mu^+\mu^-e^-\bar{\nu}_e u\bar{d} \qquad (1)$$

are considered, which differ for their content of electroweak backgrounds but are both completely unaffected by QCD backgrounds.

In the following, some details concerning the strategies followed for the calculation of the physical amplitudes and the phase space of the above $2 \to 6f$ processes will be described.

As said in the introduction, to compute the matrix elements, a recently proposed technique (`ALPHA`) has been employed. It doesn't require the evaluation of Feynman graphs and allows to obtain automatically, according to an iterative procedure, the tree-level scattering amplitudes of any given lagrangian. This is achieved by exploiting the relation between the generator of one-particle irreducible Green functions and the generator of the connected Green functions. The interested reader is referred to the original literature [14] for a detailed description of the method. Here it is worth pointing out that

- the procedure, which is entirely automatic, has been checked successfully against the precise predictions existing for the processes $e^+e^- \to 4f$ [7,9] and applied to obtain original results for the rate of the reactions $e^+e^- \to 4f + \gamma$ [15] and $\gamma\gamma \to 4$ fermions [16];
- to calculate the amplitude for a certain process, an input file is provided, where one has simply to specify the type of the process and the total number of particles involved in intial and final states. For the pure QED case the required input is an integer vector $N_{prt} \equiv (n_1,\ldots,n_6)$ where $n_1,\ldots,n_6$ are the numbers of initial e^-, final e^+, final e^-, initial e^+, initial and final photons respectively; once this vector is initialized and the proper kinematics is provided `ALPHA` returns the scattering matrix elements;[1]
- the present calculation is the first application of `ALPHA` to the computation of $e^+e^- \to 6f$ processes; this enables, in particular, to check yet untested parts of the input lagrangian (i.e. the coupling of the higgs boson to the W and Z bosons and some of the quartic nonabelian gauge boson couplings) and to show the potentials of the algorithm for multi-particle production processes involving a very large number of diagrams.

The kinematics of the $2 \to 6f$ processes has been treated generating the 6-body phase space recursively. This choice is particularly useful since processes where a particle decays into other particles which subsequently decay are being considered (see Fig. 1). In particular, denoting by $p_{-(+)}$ the four-momentum of the incoming electron (positron), q_i, $i = 1,\ldots,6$, the final-state outgoing four-momenta and $P = p_- + p_+$, the phase space can be written as

---

[1] For the standard model the only difference is that the vector N_{prt} has much more entries (a pair for each SM particle)
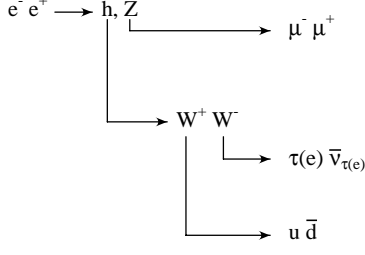
Fig. 1. The decay chain in the channel $e^+e^- \to \mu^+\mu^- u\bar{d}\tau^-(e^-)\bar{\nu}_{\tau(e)}$

Fig. 2. The Feynman diagram for the Higgs boson signal in the channel $e^+e^- \to \mu^+\mu^- u\bar{d}\tau^-(e^-)\bar{\nu}_{\tau(e)}$

$$d\Phi_6(P; q_1, \ldots, q_6)$$
$$= (2\pi)^{12} d\Phi_2(P; Q_Z, Q_h) d\Phi_2(Q_Z; q_1, q_2)$$
$$d\Phi_2(Q_h; Q_{W^+}, Q_{W^-}) d\Phi_2(Q_{W^+}; q_3, q_4)$$
$$d\Phi_2(Q_{W^-}; q_5, q_6) dQ_Z^2 dQ_h^2 dQ_{W^+}^2 dQ_{W^-}^2, \qquad (2)$$

where $Q_Z = q_1 + q_2$, $Q_h = \sum_{i=3}^6 q_i$, $Q_{W^+} = q_3 + q_4$ and $Q_{W^-} = q_5 + q_6$. Globally, fourteen independent variables (including a trivial overall azimuthal angle) are required; they have been chosen according to the following scheme:

- four invariant masses Q_Z^2, Q_h^2, $Q_{W^+}^2$, Q_{W^-}
- five ϑ- and φ-angle pairs, in the rest frame of each decaying "particle", namely in the frames where $\mathbf{P} = 0$, $\mathbf{Q}_Z = 0$, $\mathbf{Q}_h = 0$, $\mathbf{Q}_{W^+} = 0$ and $\mathbf{Q}_{W^-} = 0$, respectively; once these variables are generated, the four-momenta of the outgoing fermions are derived in each "rest" frame and then boosted back to the laboratory frame.

The choice of the kinematics has been motivated by the dynamics of the Higgs boson signal; the same phase space is also conveniently employed for the background processes.

In order to obtain reliable phenomenological results for the energies of the future e^+e^- colliders, the lowest-order calculation of the matrix elements has to be supplemented with the potentially large effects of energy losses due to the emission of initial state photons, caused by the mutual interaction of the colliding electrons and positrons at the "parton" level (bremsstrahlung or ISR), as well as to the synchrotron radiation generated by the strong electromagnetic interaction between dense bunches of particles (beamstrahlung). Both the contribution of ISR and beamstrahlung have been incorporated in the physics simulation in order to provide as realistic as possible predictions. The task has been accomplished by interfacing ALPHA with the Monte Carlo program HIGGSPV/WWGENPV, properly adapted to treat $6f$ production processes. This allowed to exploit as much as possible the expertise developed in the context of the LEP2 workshop [19], concerning 4-fermion production processes. In particular, the method of QED structure functions (SF) [28] is used to account for ISR according to the factorized formula

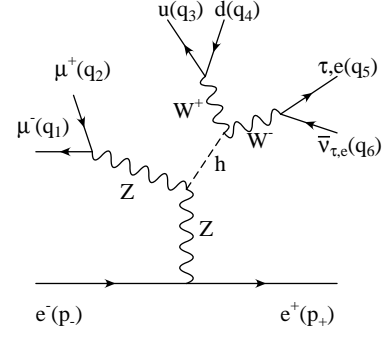$$\sigma(s) = \sum_i \int_0^1 dx_1 \, dx_2 \, D(x_1, s) D(x_2, s) d[PS] \frac{d\sigma}{d[PS]} \frac{w_i}{W},$$
$$(3)$$

where $D(x, s)$ is the electron SF, $d[PS]$ denotes the volume element of the 6-body phase space, $d\sigma/d[PS]$ is the tree-level hard scattering density in the c.m. frame, built by means of the total scattering amplitude as returned by ALPHA and of the proper jacobian factors; w_i and $W = \sum_i w_i$ are weights introduced to increase the efficiency of the Monte Carlo integration, namely by incorporating the weights w_i in the integration measure according to a multi-channel importance sampling [29]; the random number generator employed is RANLUX [30]. Beamstrahlung corrections are simulated using the parameterizations of such effects recently implemented in the library CIRCE [31], namely according to the formula

$$\sigma(s) = \sum_i \int_0^1 dz_1 dz_2 D_{BS}(z_1, z_2; \sqrt{s}) \qquad (4)$$
$$\times \int_0^1 dx_1 \, dx_2 \, D(x_1, s) D(x_2, s) d[PS] \frac{d\sigma}{d[PS]} \frac{w_i}{W},$$

where D_{BS} is the beamstrahlung distribution.[2] When ISR and/or beamstrahlung are taken into account, the four-momenta of the final-state particles are additionally boosted to the laboratory frame, in order to take into account the c.m. boost generated by such effects. At present, ISR is treated in the strictly collinear approximation.

A technical but important item in the numerical calculation is the choice of the weight functions w_i employed for the implementation of the importance sampling. This choice has to be driven by the physics involved. When considering only the Higgs boson signal (see Fig. 2), it has to be observed that muon pairs come from the Z boson decay, while the remaining four final-state fermions come from the Higgs boson decay. Moreover, the hadronic pair comes from the W^+ boson decay and the additional leptonic pair from the W^- boson decay. This means that the most populated phase space region is in the surroundings of $Q_Z^2 \simeq M_Z^2$, $Q_h^2 \simeq m_h^2$ and $Q_{W^\pm}^2 \simeq M_W^2$. When considering the leading background processes common to both

---

[2] The TESLA accelerator code has been used. The library CIRCE provides the beamstrahlung parameterization for some fixed $\sqrt{s}$, in particular $\sqrt{s} = 350$ and 500 GeV. For one of the c.m. energies considered in the following simulations, namely $\sqrt{s} = 360$ GeV, the parameterization relative to 350 GeV has been used, as explicitly allowed in the original documentation
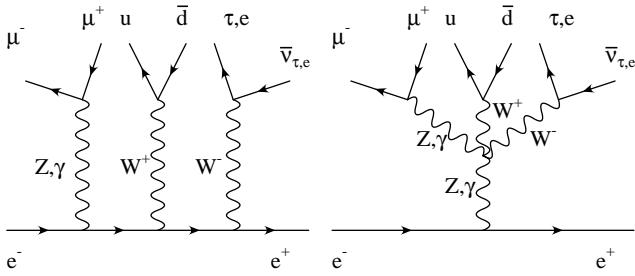
Fig. 3. Feynman diagrams for typical background processes in the channel $e^+e^- \to \mu^+\mu^- u\bar{d}\tau^-(e^-)\bar{\nu}_{\tau(e)}$
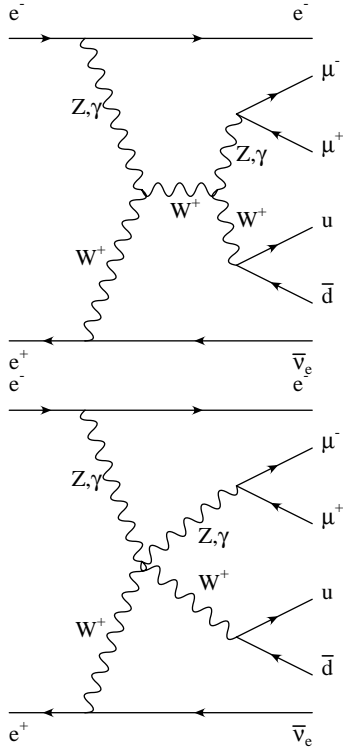

Fig. 4. Additional Feynman diagrams for typical background processes in the channel $e^+e^- \to \mu^+\mu^- u\bar{d}e^-\bar{\nu}_e$

the channels examined (see for instance Fig. 3), the muon pairs can come also, for instance, from photon conversion; moreover, Q_h^2 is no more peaked around m_h^2; the hadronic and the additional leptonic pairs still come from W's decay. At last, when considering background processes typical of the channel with the electron in the final state (see for instance Fig. 4) the $e\nu$ leptonic pair invariant mass is no more peaked around M_W^2. Following these considerations, the importance sampling adopted has the following features:

- Q_h^2 is sampled piecewise, according to a Breit-Wigner (BW) density around $Q_h^2 = m_h^2$ and a flat density elsewhere; the relative weights of the BW and flat densities are tuned according to the signal/background ratio for any given $\sqrt{s}$;
- Q_Z^2 is sampled piecewise, according to a BW density around $Q_Z^2 = M_Z^2$, according to $1/Q_Z^2$ in the lower tail and a flat density in the upper one;

- $Q_{W^\pm}^2$ are always sampled according to a BW density;
- since a realistic event selection requires a minimum scattering angle for the leptons, no particular sampling has been performed in the final-electron forward region; in particular, a minimum angle of 5° between the final electron and the incoming beams has been imposed, in such a way that the t-channel "singularity" (see for instance Fig. 4) is excluded.

The "soft-photon singularity" of the electron SF's is sampled in the standard way, as can be found in the literature [17,18].

CPU performances have not been the main concern of the study. Anyway, it is worth saying that the Monte Carlo code developed, in the worst case, generates around 3500 unweighted events in 8h CPU and, as integrator of weighted events, provides a cross section with a statistical error of around 1% in 3h CPU on a DEC ALPHA station. Such performances are sufficient for any realistic simulation.

3 Numerical results and discussion

In order to produce the numerical results shown in the present section, the input parameters used are the Fermi coupling constant G_F, the Z boson mass $M_Z = 91.1888$ GeV and the W boson mass $M_W = 80.23$ GeV. The weak mixing angle and the QED coupling constant are then computed as $\sin^2\vartheta_w = 1 - M_W^2/M_Z^2$ and $4\pi\alpha = g^2\sin^2\vartheta_w$, where $g^2 = 8M_W^2 G_F/\sqrt{2}$. Given these input parameters, all the other relevant quantities, such as the Z and W bosons widths, have been computed at the tree-level approximation and the massive boson propagators are chosen as $\sim 1/(p^2 - M^2 + i\Gamma M)$. This choice of input parameters has been performed in order to avoid problems concerning violations of the Ward identities, or, more precisely, to confine all possible gauge violation effects into the inclusion of the finite fixed widths for the massive bosons.

As far as the Higgs boson width is concerned, in the present simulation the following contributions have been taken into account: the fermionic contributions $h \to \mu\mu$, $\tau\tau, cc, bb$, where the hadronic widths have been QCD corrected taking into account the running quark mass effects [8]; the gluonic contribution $h \to gg$ according to [8]; the vector boson contribution $h \to V^*V^*$, according to [32].

The result has been tested to be $U(1)_{em}$ gauge-invariant, by comparing the results obtained with two different inverse photon propagators in the effective lagrangian implemented in ALPHA. A priori, one could expect $U(1)$ gauge invariance problems to be severe in particular in the channel with the electron in the final state. Anyway, such potential problems [33] are avoided requiring a realistic event selection, as described above. Concerning the $SU(2)$ gauge invariance, it has been pointed out in [34] that the fixed-width scheme, used in the present study, is not $SU(2)$ gauge invariant and could in principle be responsible of a bad high-energy behaviour in processes

involving six fermions in the final state. The numerical relevance of the $SU(2)$ gauge violations of the (fixed widths) results has then been checked by comparing them with results obtained in the so called "fudge scheme" [35], that is by construction gauge-invariant, and finding them compatible at the level 0.5% relative deviation.

All the numerical results, but those shown in Fig. 5, have been obtained by imposing the following *a priori* cuts: the invariant mass of the muon pair larger than 20 GeV; the invariant mass of the hadronic system larger than 10 GeV; the angle between the charged leptons and the beams larger than 5°.

The results shown in Figs. 5 and 6 have been obtained by using the program as a Monte Carlo integrator of weighted events.

Figure 5 shows the comparison between the fully extrapolated cross sections for the Higgs boson signal alone, as obtained by means of the present complete $6f$ calculation on the one hand, and within the narrow-width approximation (NWA) according to [36] on the other one. The two windows show the comparison as a function of the Higgs boson mass, for two fixed $\sqrt{s} = 360$ and 500 GeV, and as a function of the c.m. energy, for three fixed Higgs boson masses $m_h = 150$, 160 and 170 GeV, respectively. In both cases the relative deviation $\sigma_{6f}/\sigma_{NWA} - 1$ is considered. In particular, in the first plot two cases are considered, namely the case in which the total Higgs boson decay width has been used in the full $6f$ calculation (solid and dashed lines), and the case in which the Higgs boson width in the full $6f$ calculation is identified with $\Gamma(h \to W^*W^*)$ (dotted and sparsely dotted lines). The dotted and sparsely dotted lines approach zero in the region of "small" Higgs boson masses: this represents a check that the $6f$ calculation reproduces the results already present in the literature for the NWA. The solid and dashed lines do not approach zero, because of the presence of the fermionic and gluonic contributions to the total Higgs boson width, but this is the realistic case. Anyway, the off-shellness effects are contained within a few per cent, as can be also seen in the second plot.

Figure 6 shows the comparison, at the tree-level approximation, between the full cross section, the separate contribution of the Higgs boson signal and the background only, for two values of the Higgs boson mass $m_h = 150$, 170 GeV and as a function of the c.m. energy. The first plot shows the results for the channel $e^+e^- \to \mu^+\mu^-\tau^-\bar{\nu}_\tau u\bar{d}$, the second one for the channel $e^+e^- \to \mu^+\mu^-e^-\bar{\nu}_e u\bar{d}$. As a first comment, it has to be noticed that, for the event selection considered, the channel containing the electron in the final state is not very much different from the one containing the τ lepton; this in spite of the fact that the electron channel receives contributions also from t-channel processes of the kind shown in Fig. 4. The t-channel background processes start to become visible only in the high-energy tail of the plot, say around $\sqrt{s} \simeq 500$ GeV. The statistical error due to the numerical integration is of the order of 0.5% and hence invisible for the scale adopted in the plots. In both channels, the full calculation is consistent with the incoherent sum of signal and background,

at the statistical level considered. Signal/background interference effects can become relevant for resolutions better than 1%. It has to be noticed that, in both cases, $\sqrt{s} \simeq 500$ GeV represents the turning point, after which the background processes become larger than the signal for the cuts considered. It has been checked that, in the channel $e^+e^- \to \mu^+\mu^-\tau^-\bar{\nu}_\tau u\bar{d}$, the high-energy behaviour of the cross section is in good agreement with the one found in [37]. For $\sqrt{s} = 360$ and 500 GeV also the combined effect of ISR and beamstrahlung has been studied. For the full signal+background inclusive cross sections, radiative effects turn out to be confined within a few per cent, being dominated by ISR. This can be easily understood, since the Born approximation inclusive cross section is almost flat, as a function of $\sqrt{s}$, above, say, 300 GeV.

The results shown in Figs. 7–13 correspond to $\sqrt{s} = 360$ GeV, except for Figs. 8 and 13, where $\sqrt{s} = 500$ GeV. They have been obtained by analyzing the six-fermion unweighted event samples simulated by using the program as a generator. In all the cases, the number of events shown is normalized to a fixed integrated luminosity, in order to perform a comparison consistent with the corresponding cross sections. The channel $e^+e^- \to \mu^+\mu^-e\bar{\nu}_e u\bar{d}$ has been considered. As general comments, in these figures the dotted histograms represent the Born approximation results, the dashed ones represent the results including the effect of ISR and the solid ones represent the full prediction, including also the effect of beamstrahlung. It has to be noticed that, among the various distributions shown, the only ones that are very sensitive to the effect of ISR and/or beamstrahlung are the ones analyzed in Figs. 7 and 8.

The distributions shown starting from Fig. 7 have been produced by using the full $6f$ calculation for three values of the Higgs boson mass, namely $m_h = 150$, 160 and 170 GeV, and for the background only ($m_h \to \infty$).

Figure 7 shows the distribution of the missing mass, defined as $M_{miss} = \sqrt{(P - Q_Z)^2}$, P being the total incoming nominal four-momentum, i.e. before the energy losses due to ISR and/or beamstrahlung, and Q_Z being the muon pair total four momentum $q_1 + q_2$ (see (2)). In the absence of radiative effects, the missing mass coincides with the invariant mass of the Higgs boson decay products. This is an experimentally relevant quantity, since the Higgs boson width is too tiny to be resolved directly. The radiative effects amount generically to populate the high-mass tails of the distribution. A comparison between Figs. 7 and 8 shows that such effect is larger at $\sqrt{s} = 500$ GeV.

In Fig. 9 the invariant mass of the μ pair system $(M_{\mu^+\mu^-} = \sqrt{(q_1 + q_2)^2})$ is shown, in a window of some Z boson widths around the Z boson mass. The distribution is always peaked at the Z boson mass; the presence of the Higgs boson signal is revealed by the height of the peak, which is enhanced by a factor of about 6 with respect to the background.

Figure 10 shows the distribution of the angle between the total $\mu^+\mu^-$ three-momentum and the beam, in the laboratory frame. In the presence of the Higgs boson signal only, it coincides with the Z boson scattering angle.
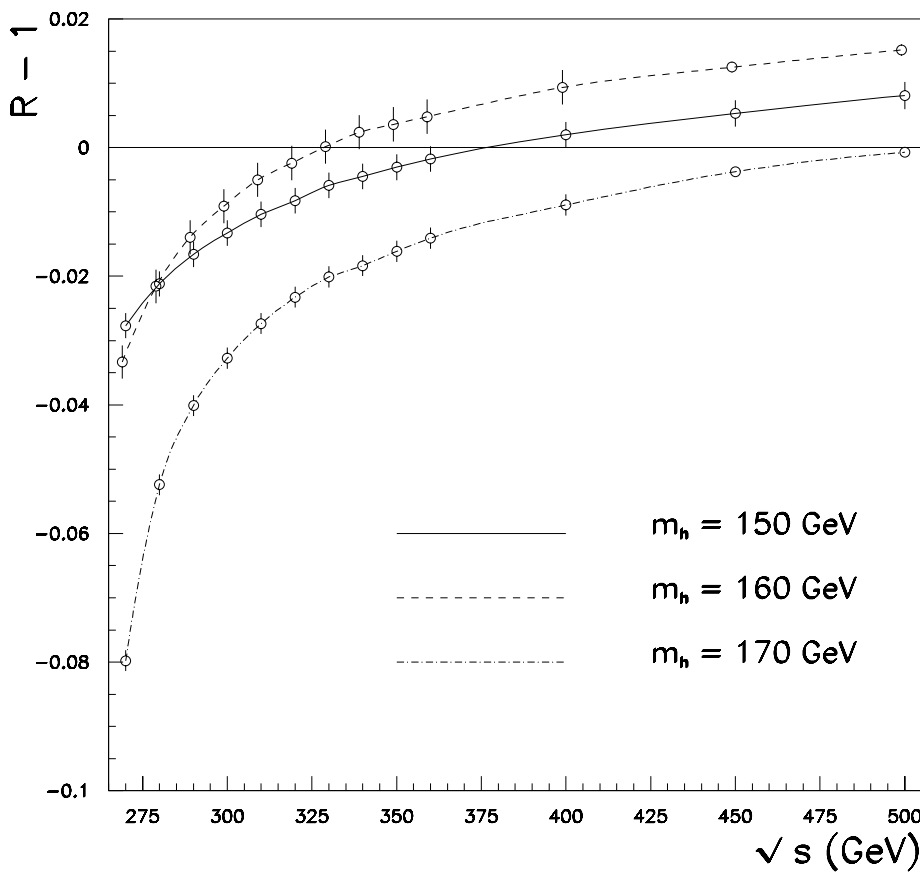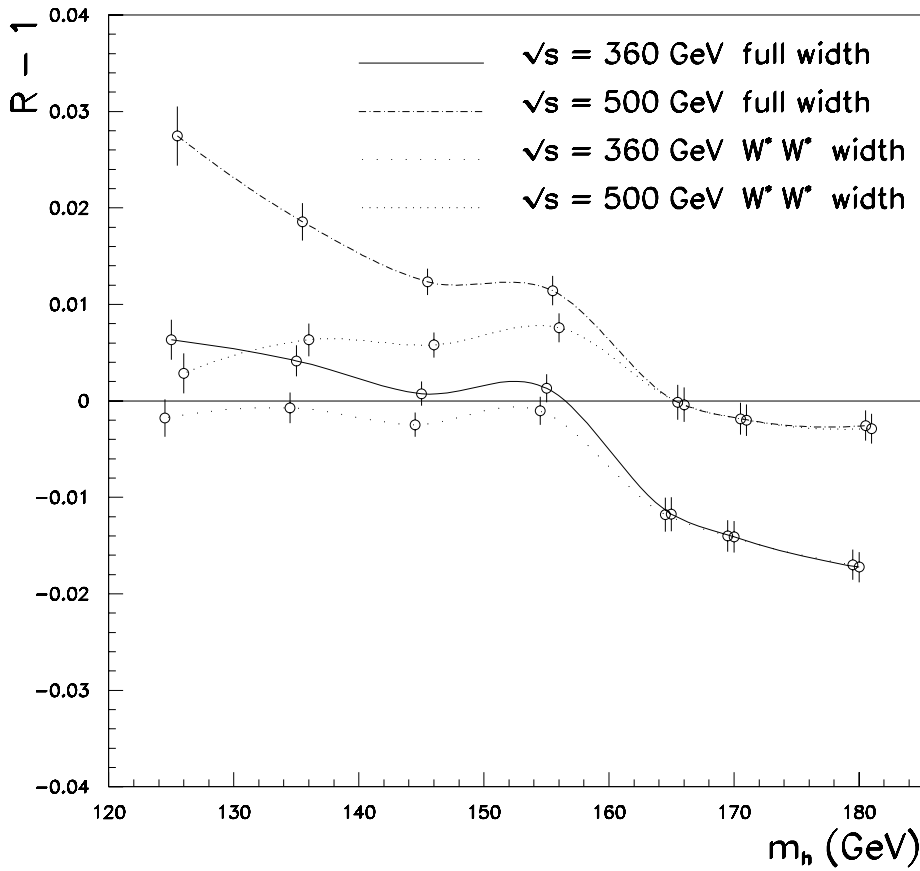
Fig. 5. The comparison between the results of the full six fermion simulation and the results obtained in the narrow-width approximation, as function of the Higgs boson mass m_h and of the c.m. energy. R is defined as $R = \sigma_{6f}/\sigma_{NWA}$; for more details on the widths see the text (Sect. 3)
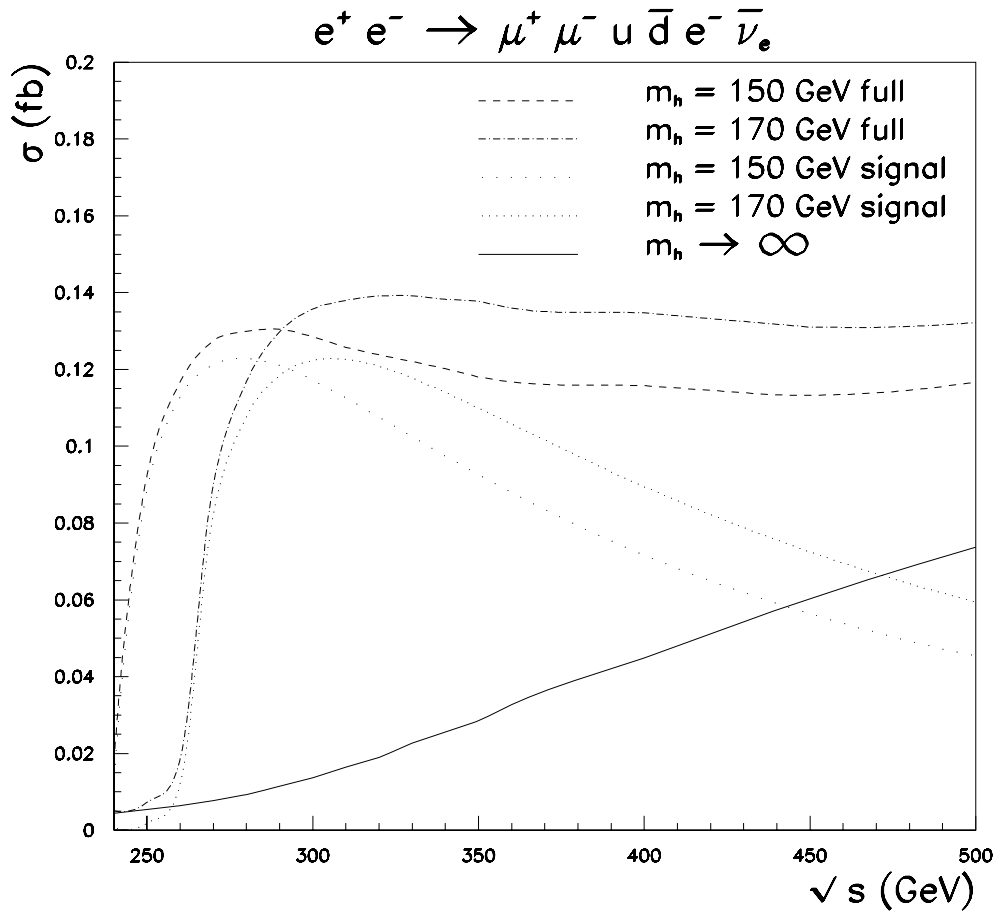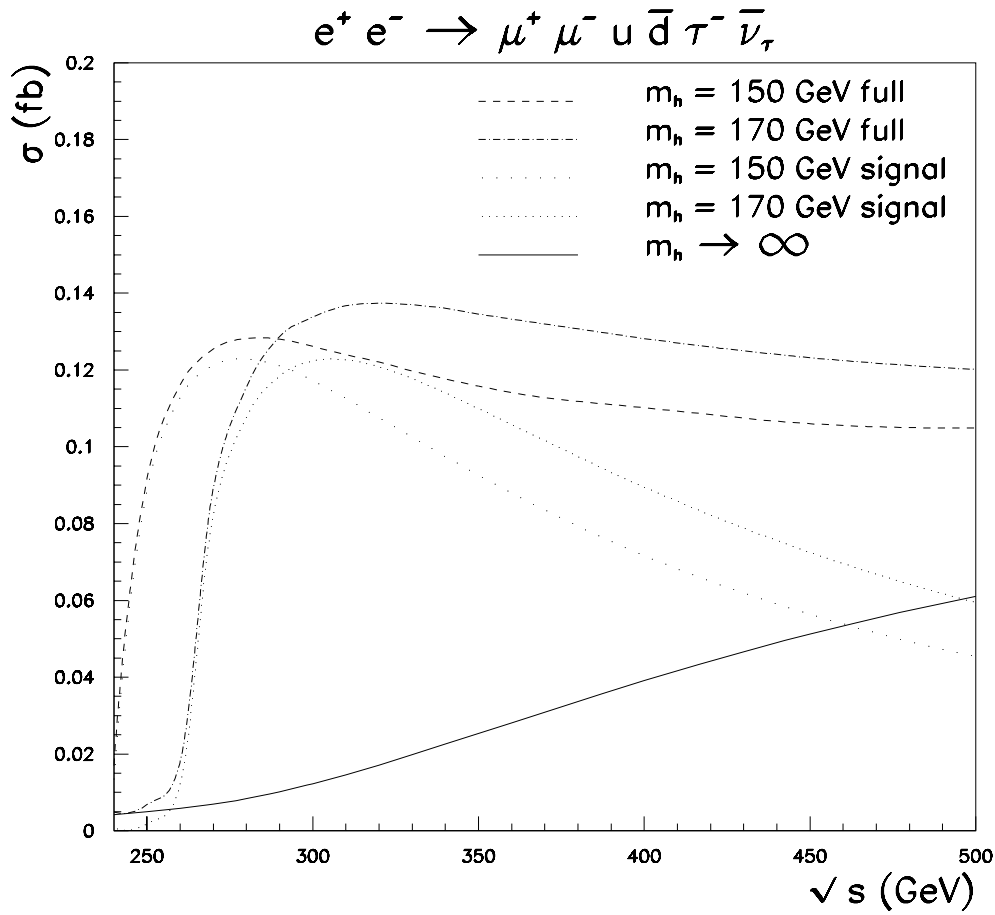
Fig. 6. The cross sections for the channels $e^+e^- \to \mu^+\mu^-\tau^-\bar{\nu}_\tau u\bar{d}$ and $e^+e^- \to \mu^+\mu^-e^-\bar{\nu}_e u\bar{d}$ as functions of the c.m. energy. Full $6f$ cross sections for $m_h = 150$ and 170 GeV (*dashed* and *dash-dotted lines*, respectively), Higgs boson signals only (*sparsely dotted* and *dotted lines*, respectively) and background only (*solid lines*)
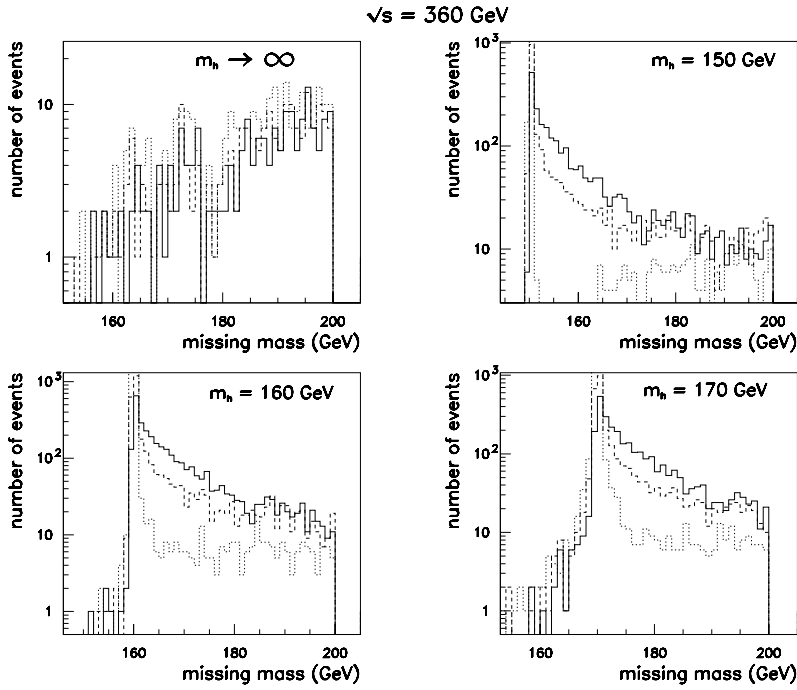
Fig. 7. The missing mass distributions $M_{miss} = \sqrt{(P - Q_Z)^2}$, P being the total incoming nominal four-momentum, and Q_Z being the muon pair total four momentum, at $\sqrt{s} = 360$ GeV. *Dotted, dashed* and *continuous histograms* correspond to Born approximation, Born+ISR and Born+ISR+beamstrahlung results, respectively
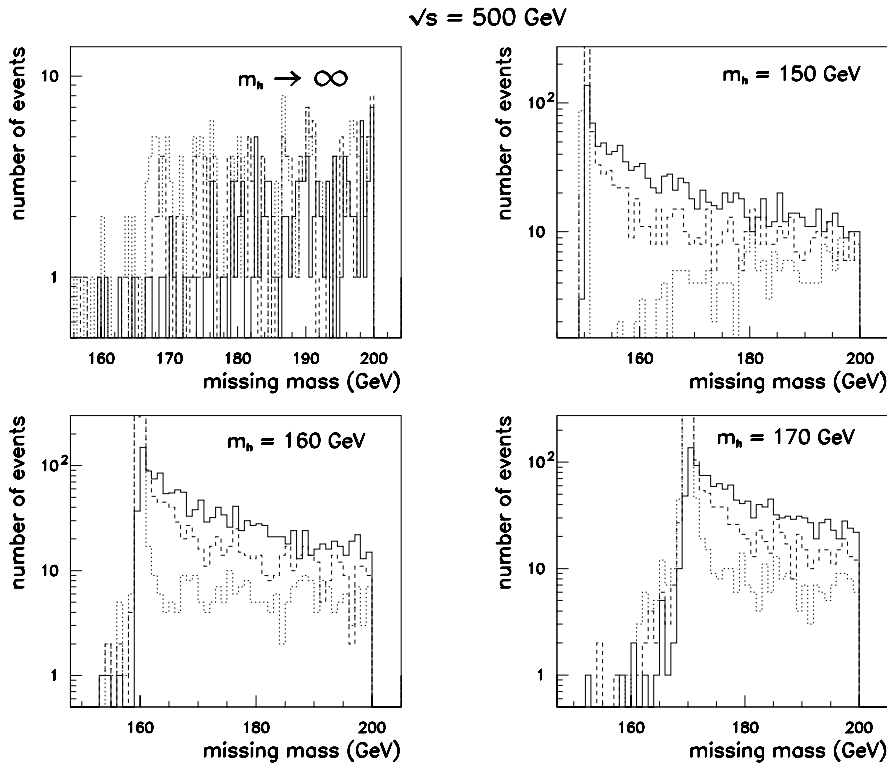

Fig. 8. The missing mass distributions at $\sqrt{s} = 500$ GeV. Notation as in Fig. 7

As the Higgs boson mass varies, the distributions are quite similar, all smoothly peaked around $\vartheta_\mu = \pi/2$. The presence of the Higgs boson signal is revealed by the height of the peak also in this case.

In Fig. 11 the distribution of the variable $\xi_1 = (\cos \vartheta^*_{eu} + \cos \vartheta^*_{ed})/2$ is shown. The angles ϑ^* are defined as follows. First, the $\bar{\nu}_e$ "three-momentum" is reconstructed as $\mathbf{v}_6 = -\sum_{i=1}^{5} \mathbf{q}_i$ and its energy component is defined by

means of the shell relation $v_6^0 = |\mathbf{v}_6|$. v_6 coincides with the true $\bar{\nu}_e$ four-momentum only in the Born approximation; in the presence of radiative effects in the collinear approximation $\mathbf{v}_6$ is the total lost three-momentum. Then the four vector h defined as $h = q_3 + q_4 + q_5 + v_6$ is considered; in the Born approximation and in the presence of the Higgs boson signal only, it coincides with the Higgs boson four-momentum. The angles ϑ^* are measured in the reference
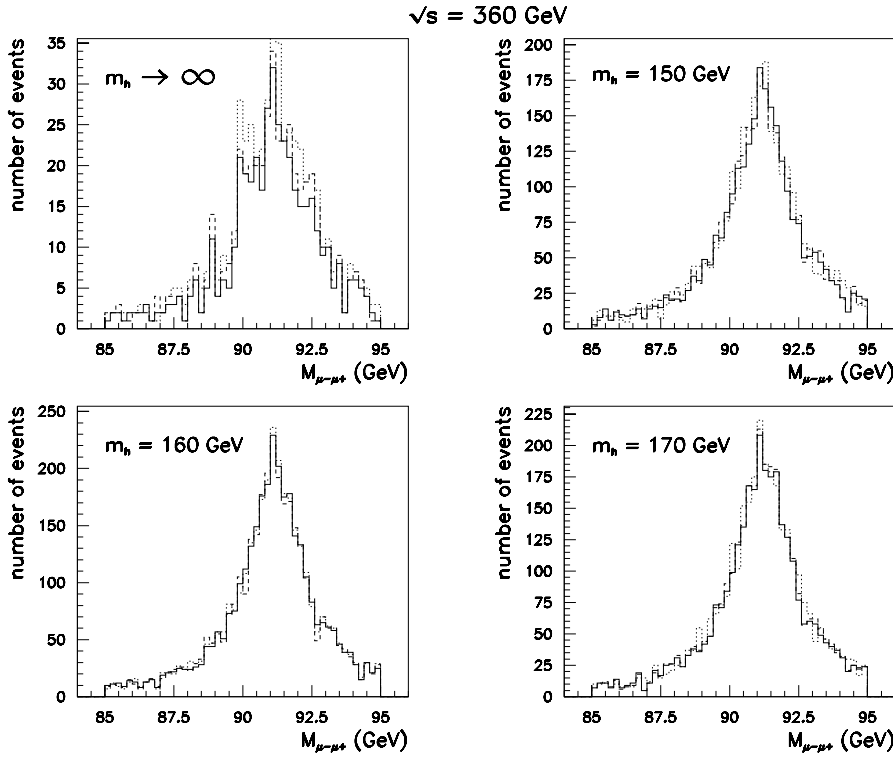
Fig. 9. The μ-pair invariant mass distribution, $M_{\mu^+\mu^-} = \sqrt{(q_1 + q_2)^2}$, in the surroundings of $M_{\mu^+\mu^-} = M_Z$ at $\sqrt{s} = 360$ GeV. Notation as in Fig. 7
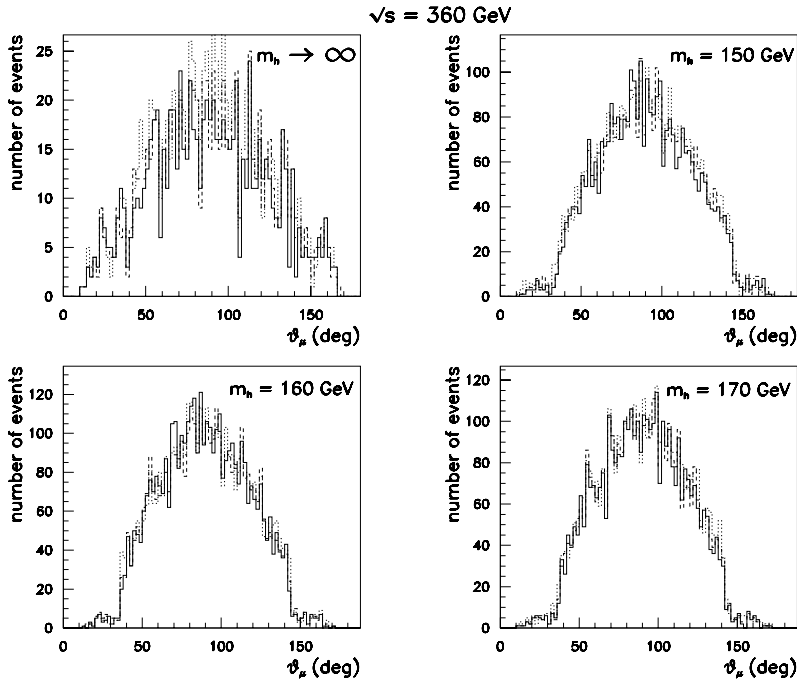

Fig. 10. The distribution of the angle between the total μ-pair three-momentum and the beam, in the laboratory frame, at $\sqrt{s} = 360$ GeV. Notation as in Fig. 7

frame in which $\mathbf{h} = \mathbf{0}$; in the Born approximation and in the presence of the Higgs boson signal alone, it is the rest frame of the Higgs particle. In the presence of the Higgs boson signal, the distribution of ξ_1 sharpens around zero. In the above procedure, there is an obvious arbitrariness in defining v_6^0; actually, it could also be defined by means of the energy-momentum conservation, in such a way that v_6 is the total lost four momentum. It has been checked

that the results are not critical with respect to this choice. It has to be noticed that the variable ξ_1 is a particularly sensitive variable; in fact, the presence of the Higgs boson signal is revealed by a significant change in the shape of the distribution.

Figures 12 and 13 show the distributions of the variable ξ_2 defined in an analogous way to ξ_1 as $\xi_2 = \mathbf{q}_5^* \cdot \mathbf{Q}_{had}^* / q_5^{0*} / Q_{had}^{0*}$, where q_5^* and Q_{had}^* are the four-momenta
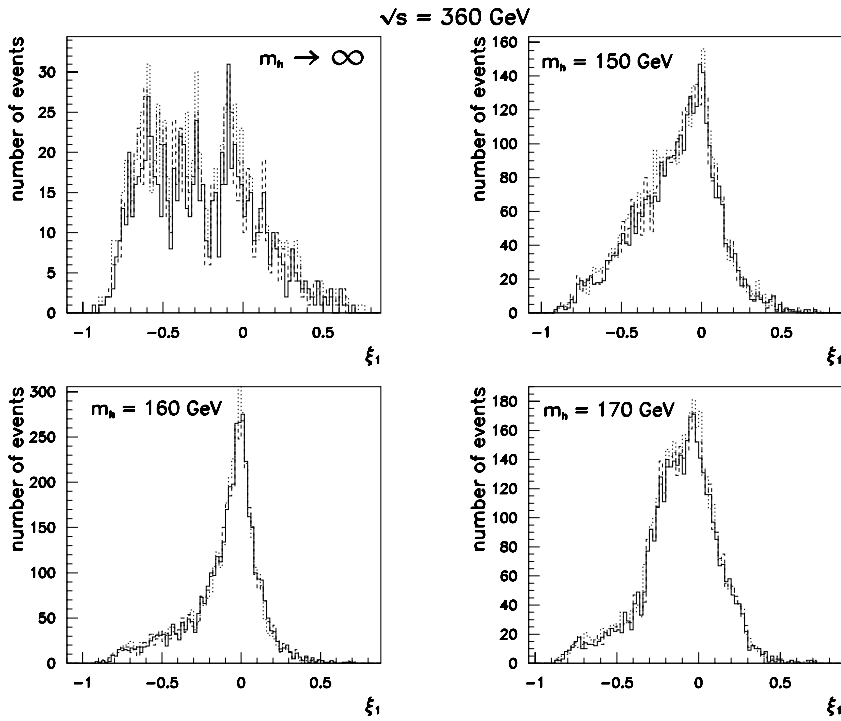
Fig. 11. The distribution of the variable ξ_1 (see the text for the definition, Sect. 3) at $\sqrt{s} = 360$ GeV. Notation as in Fig. 7
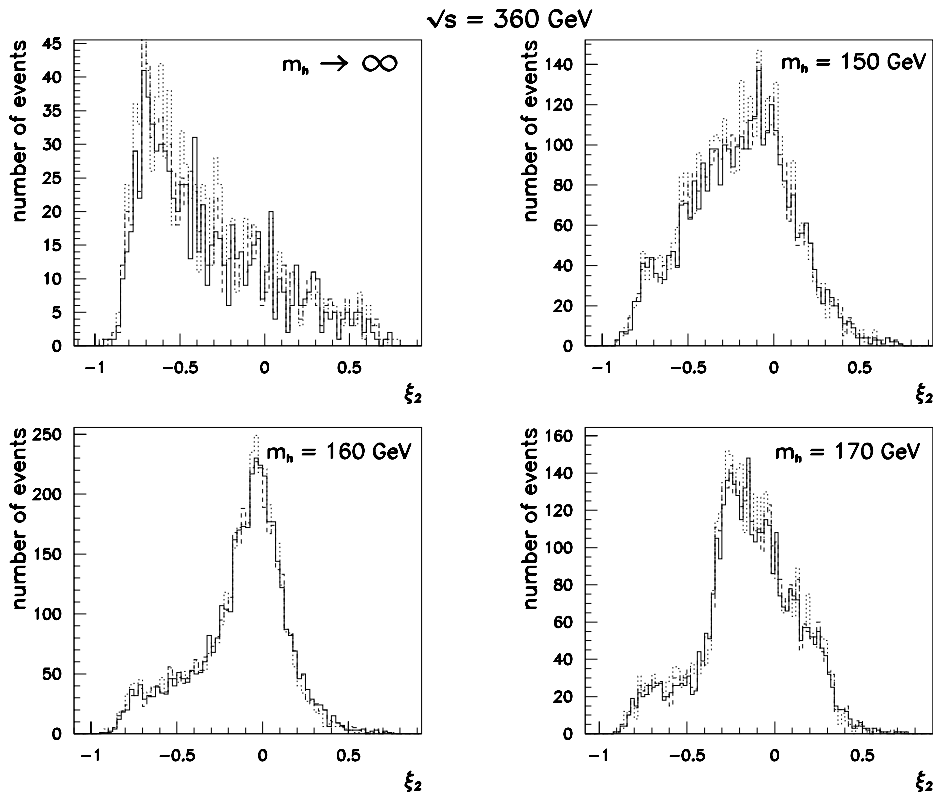

Fig. 12. The distribution of the variable ξ_2 (see the text for the definition, Sect. 3) at $\sqrt{s} = 360$ GeV. Notation as in Fig. 7
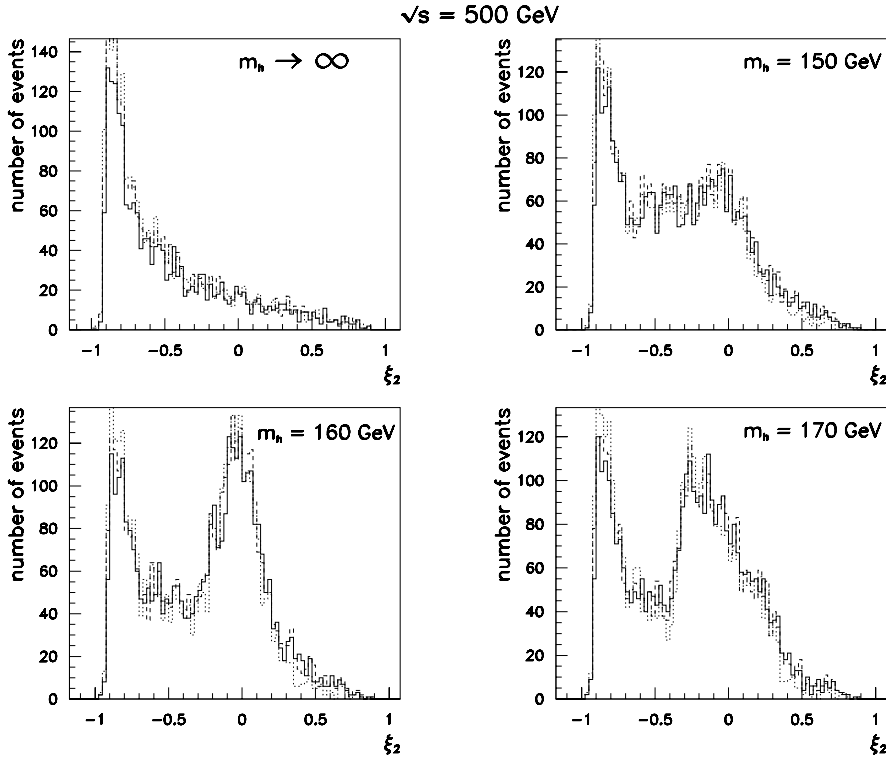
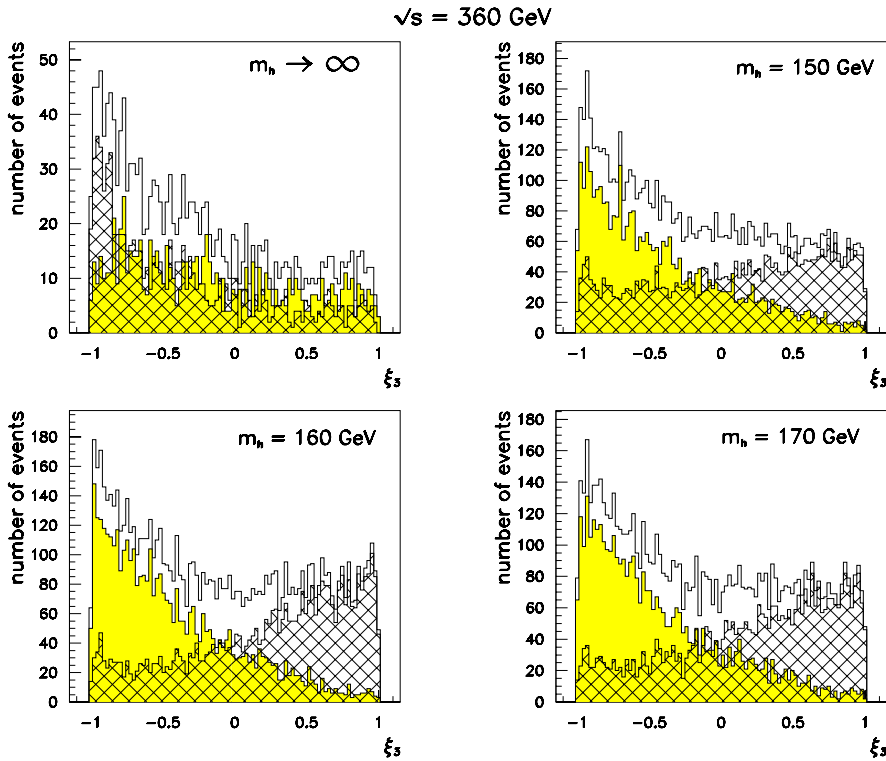**Fig. 13.** The same as Fig. 12 at $\sqrt{s} = 500$ GeV. Notation as in Fig. 7

Fig. 14. The distribution of the variable ξ_3 (see the text for the definition, Sect. 3) at $\sqrt{s} = 360$ GeV. All the histograms include the effect of ISR and beamstrahlung. The *shaded* and *hatched histograms* represent $\cos \vartheta^*_{eu}$ and $\cos \vartheta^*_{ed}$; the *white histogram* is the sum of the previous ones

of the outgoing electron and hadronic system, respectively, in the reference frame defined above. Incidentally, Q_{had} coincides with the W^+ boson four-momentum. The c.m. energies considered are $\sqrt{s} = 360$ and 500 GeV. For both the c.m. energies, the variable ξ_2 shows an enhanced sen-

sitivity to the presence of the Higgs boson particle. Actually, the background distribution has a more pronounced peak in the region $\xi_2 \simeq -1$. It has to be noticed that at $\sqrt{s} = 500$ GeV there is a two-peak structure, where the peak around $\xi_2 \simeq 0$ is due to the Higgs boson signal,
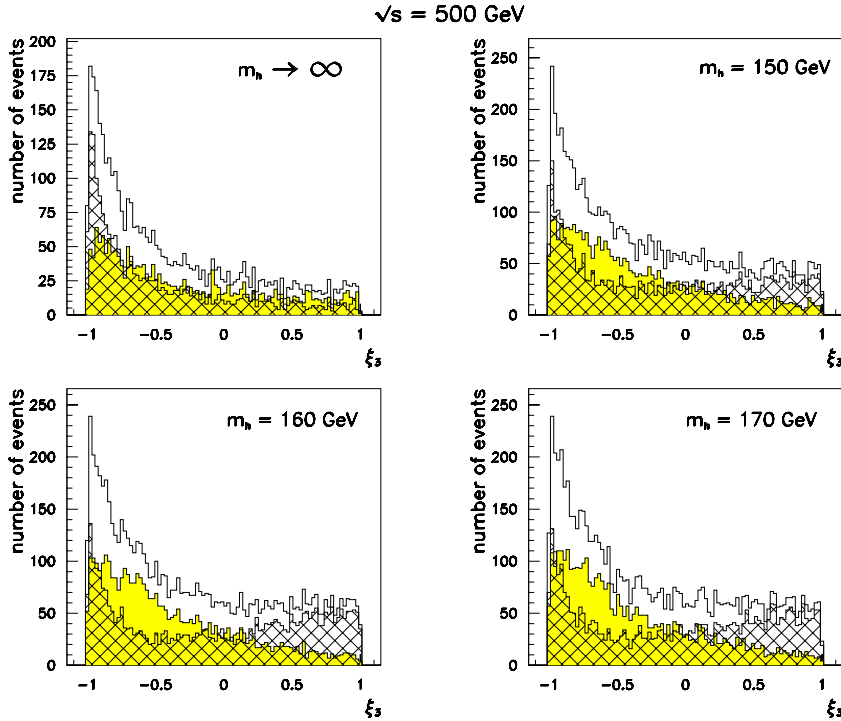
Fig. 15. The same as Fig. 14 at $\sqrt{s} = 500$ GeV. Notation as in Fig. 14

whereas the one at $\xi_2 \simeq -1$ is due to the background processes, which in this case give a contribution to the cross section comparable to the signal contribution (see Fig. 6).

The shapes of the variables $\xi_{1,2}$ are very sensitive to the presence of the Higgs boson signal. However, they are only partly determined by the underlying dynamics: in fact they are not sensitive to the spinless nature of the Higgs particle. In order to point out the spinless nature of the Higgs boson, it is necessary to investigate more exclusive forms of angular correlations. To this aim, the variable ξ_3 has been defined as $\cos\vartheta^*_{eu}$ or $\cos\vartheta^*_{ed}$, i.e. the cosine of the angle between the charged lepton and the *up*- or *down*-quark in the reference frame defined above. Figures 14 and 15 show the distribution of the two cosines for $\sqrt{s} = 360$ GeV and 500 GeV, respectively. In all the histograms the effect of ISR and beamstrahlung have been included. The shaded and hatched histograms represent $\cos\vartheta^*_{eu}$ and $\cos\vartheta^*_{ed}$, respectively. The white histogram represents the sum of the previous histograms. In all the cases, $\cos\vartheta^*_{eu}$ is peaked at -1, both in the presence and in the absence of the Higgs boson signal. On the contrary, $\cos\vartheta^*_{ed}$ is peaked at -1 in the presence of the background processes only, whereas in the presence of the Higgs boson signal the region $\cos\vartheta^*_{ed} \simeq 1$ is significantly populated. The shapes of the variables ξ_3 are sensitive to the spinless nature of the Higgs particle. Such a property has been pointed out also in a recent paper [38], as a useful tool in the search for the Higgs boson in the decay channel $h \to W^+W^- \to l^+l'^-\nu_l\bar{\nu}_{l'}$ at the LHC. Anyway, in that paper the study has been performed on signal and background separately, without relying upon a full multiparticle calculation. It is worth noting that the sensitivity of the shape is definitely larger at $\sqrt{s} = 360$ GeV rather

than at $\sqrt{s} = 500$ GeV, where signal and background are of the same order (see Fig. 6).

4 Conclusions and outlook

The production of a Standard Model Higgs boson in e^+e^- collisions at very high energies has been studied, considering the case of intermediate-mass Higgs boson which yields a six-fermion final state. The calculation of the Higgs boson signal as well as of the background matrix elements has been carried out using the automatic algorithm `ALPHA`, which reveals to be particularly powerful for such six-fermion calculations involving in the conventional diagrammatic approach a huge number of graphs. The tree-level scattering amplitudes returned by `ALPHA` have been corrected for the effects of bremsstrahlung and beamstrahlung, in order to provide as comprehensive as possible results, by interfacing `ALPHA` with the Monte Carlo program `HIGGSPV/WWGENPV`, properly adapted to treat $6f$ production processes.

As a summary of the main outcomes of the study, the following items have to be pointed out:

- the full $6f$ calculation as compared with the calculation carried out within the narrow-width approximation shows that the various off-shellness effects can be of the order of some per cent; for experimental accuracies better that some per cent the narrow-width approximation becomes inadequate;
- the full calculation as compared to the incoherent sum of signal and background reveals that, for the channels considered, signal/background interference effects are

compatible with zero at the level of precision of about 0.5%;

- the missing mass distribution, relevant for the determination of the Higgs boson mass, is strongly affected by initial-state radiation and/or beamstrahlung effects (radiative effects), as expected;
- the shapes of all the other distributions considered in the paper are only smoothly affected by radiative effects;
- the variables that are mostly sensitive to the presence of the Higgs particle decaying into a W-boson pair are ξ_1 and ξ_2 of Figs. 11, 12 and 13; the variable most sensitive to the spinless nature of the Higgs boson is ξ_3 of Figs. 14 and 15; in all the cases, they are variables concerning the spin correlations of the Higgs boson decay products, and can be meaningfully analyzed only by means of a complete $6f$ calculation.

As a conclusion, the approach described in the present paper represents a valuable tool for Higgs boson searches at NLC and, more generally, for the study of scattering processes involving multi-particle production.

References

1. J. Casas, J. Espinosa and M. Quiros, Phys. Lett. **B342** (1995) 171; G. Altarelli and G. Isidori, Phys. Lett. **B377** (1994) 141; M. Lindner, Z. Phys. **C31** (1986) 295; M. Sher, Phys. Rep. **179** (1989) 273; N. Cabibbo, L. Maiani, G. Parisi and R. Petronzio, Nucl. Phys. **B158** (1979) 295

2. LEP Electroweak Working Group, R. Clare et al., CERN-PPE/96-183; A. Blondel, Proc. of the XXVIII Intern. Conf. on High Energy Physics, Warsaw, 1996

3. ATLAS Technical Proposal, CERN/LHC/94-43 LHCC/P2 (December 1994); CMS Technical Proposal, CERN/LHC/94-43 LHCC/P1 (December 1994)

4. Z. Kunszt, "Theoretical Aspects of Higgs Hunting at LHC", `hep-ph/9704263`; Z. Kunszt, S. Moretti and W.J. Stirling, "Higgs Production at the LHC: an Update on Cross Sections and Branching Ratios", `hep-ph/9611397`

5. T. Ohl, "Electroweak Event Generators for LEP2 and the Linear Collider", IKDA 96/21, in Proceedings of CRAD'96, Third International Symposium on Radiative Corrections, Cracow, August 1-5, 1996

6. F. Berends, W. Beenakker et al., "WW Cross Sections and Distributions", in Physics at LEP2, G. Altarelli, T. Sjöstrand and F. Zwirner, eds., CERN Report **96-01** (Geneva, 1996), vol. 1, p. 79

7. F. Boudjema, B. Mele et al., "Standard Model Processes", in Physics at LEP2, G. Altarelli, T. Sjöstrand and F. Zwirner, eds., CERN Report **96-01** (Geneva, 1996), vol. 1, p. 207

8. M. Carena, P.M. Zerwas et al., "Higgs Physics", in Physics at LEP2, G. Altarelli, T. Sjöstrand and F. Zwirner, eds., CERN Report **96-01** (Geneva, 1996), vol. 1, p. 351

9. D. Bardin, R. Kleiss et al., "Event Generators for WW Physics", in Physics at LEP2, G. Altarelli, T. Sjöstrand and F. Zwirner, eds., CERN Report **96-01** (Geneva, 1996), vol. 2, p. 3

10. M.L. Mangano, G. Ridolfi et al., "Event Generators for Discovery Physics", in Physics at LEP2, G. Altarelli, T. Sjöstrand and F. Zwirner, eds., CERN Report **96-01** (Geneva, 1996), vol. 2, p. 299

11. E. Accomando, S. Ballestrero and M. Pizzio, "Semileptonic six fermion processes at future e^+e^- colliders: signal and irreducible background for top and WWZ physics", Torino preprint DFTT 74/96; E. Accomando, talk given at the ECFA/DESY LC Workshop, DESY, Hamburg, November 21, 1996

12. F. Yuasa and Y. Kurihara, private communication, KEK preprint 97-42

13. K. Hagiwara and D. Zeppenfeld, Nucl. Phys. **B313** (1989) 560

14. F. Caravaglios and M. Moretti, Phys. Lett. **B358** (1995) 332

15. F. Caravaglios and M. Moretti, "e^+e^- into Four Fermions plus γ with ALPHA", `hep-ph/9604316`, to appear in Z. Phys. **C**

16. M. Moretti, Nucl. Phys. **484** (1996) 3

17. Program `HIGGSPV`, by G. Montagna, O. Nicrosini and F. Piccinini; write up in [9] and [10]

18. Program `WWGENPV`, by G. Montagna, O. Nicrosini and F. Piccinini; write up in [9] and [10]; see also G. Montagna, O. Nicrosini and F. Piccinini, Comput. Phys. Commun. **90** (1995) 141; D.G. Charlton, G. Montagna, O. Nicrosini and F. Piccinini, Comput. Phys. Commun. **99** (1997) 355

19. Physics at LEP2, G. Altarelli, T. Sjöstrand and F. Zwirner, eds., CERN Report **96-01** (Geneva, 1996), vols. 1 and 2

20. J.F. Gunion, "Detecting and Studying Higgs Bosons", `hep-ph/9705282`

21. S. Dawson, "The Standard Model Intermediate Mass Higgs Boson", `hep-ph/9703387`

22. H. Haber et al., "Weakly-Coupled Higgs Bosons and Precision Elewctroweak Physics", `hep-ph/9703391`

23. A. Djouadi, "Higgs Phenomenology: a Short Review", `hep-ph/9612361`

24. P.M. Zerwas, in Proc. of Les Recontres de la Vallée d'Aoste, La Thuile 1994, M. Greco ed. (Edition Frontiéres)

25. H. Murayama and M.E. Peskin, "Physics Opportunities of e^+e^- Linear Colliders", `hep-ex/9606003`

26. S. Moretti, `hep-ph/9611432`; Z. Phys. **C71** (1996) 267; Phys. Rev. **52** (1995) 6316

27. A. Ballestrero, E. Maina and S. Moretti, Phys. Lett. **B333** (1994) 434

28. E.A. Kuraev and V.S. Fadin, Sov. J. Nucl. Phys. **41** (1985) 466; G. Altarelli and G. Martinelli, in Physics at LEP, J. Ellis and R. Peccei, eds., CERN Report **86-02** (Geneva, 1986), vol. 1, p. 47; O. Nicrosini and L. Trentadue, Phys. Lett. **B196** (1987) 551

29. F. James, Rep. Prog. Phys. **34** (1980) 1145

30. F. James, Comput. Phys. Commun. **79** (1994) 111

31. T. Ohl, IKDA-96-13, `hep-ph/9607454`, in press on Comput. Phys. Commun

32. B. Kniehl, Phys. Lett. **B244** (1990) 537
33. E.N. Argyres et al., Phys. Lett. **B358** (1995) 339
34. W. Beenakker et al., `hep-ph/9612260`
35. U. Baur and D. Zeppenfeld, Phys. Rev. Lett. **75** (1995) 1002; Y. Kurihara, D. Perret-Gallix and Y. Shimizu, Phys. Lett. **B349** (1995) 367; U. Baur, J.A.M. Vermaseren and D. Zeppenfeld, Nucl. Phys. **B375** (1992) 3
36. P.M. Zerwas, DESY preprint 93-001
37. V. Barger, T. Han and R.J.N. Phillips, Phys. Rev. **D39** (1989) 146
38. M. Dittmar and H. Dreiner, "$h \to W^+W^- \to l^+l'^-\nu_l\bar{\nu}_{l'}$ as the Dominant SM Higgs Search at the LHC for $M_h = 155 - 180$ GeV", `hep-ph/9703401`